

## Some exact results for Boltzmann's annihilation dynamics

François Coppex,<sup>1</sup> Michel Droz,<sup>1</sup> Jarosław Piasecki,<sup>2</sup> Emmanuel Trizac,<sup>3</sup> and Peter Wittwer<sup>1</sup>

<sup>1</sup>*Department of Physics, University of Genève, CH-1211 Genève 4, Switzerland*

<sup>2</sup>*Institute of Theoretical Physics, University of Warsaw, PL-00 681 Warsaw, Poland*

<sup>3</sup>*Laboratoire de Physique Théorique, Bâtiment 210, Université de Paris-Sud, 91405 Orsay, France*

(Received 17 October 2002; published 12 February 2003)

The problem of ballistic annihilation for a spatially homogeneous system is revisited within Boltzmann's kinetic theory in two and three dimensions. Analytical results are derived for the time evolution of the particle density for some isotropic discrete bimodal velocity modulus distributions. According to the allowed values of the velocity modulus, different behaviors are obtained: power law decay with nonuniversal exponents depending continuously upon the ratio of the two velocities, or exponential decay. When one of the two velocities is equal to zero, the model describes the problem of ballistic annihilation in the presence of static traps. The analytical predictions are shown to be in agreement with the results of two-dimensional molecular dynamics simulations.

DOI: 10.1103/PhysRevE.67.021103

PACS number(s): 45.05.+x

### I. INTRODUCTION

In ballistically controlled reactions, particles with a given initial velocity distribution move freely (ballistic motion) in a  $d$ -dimensional space. When two of them meet, they annihilate and disappear from the system. This apparently simple problem has attracted a lot of attention during the past years [1–14] for the following reasons. First, this is one of the few problems of nonequilibrium statistical physics that can be exactly solved in some cases, and second it models some growth and coarsening processes [15].

This field was entered with the pioneering work by Elskens and Frisch [1], where a one-dimensional system with only two possible velocities  $+c$  or  $-c$  was studied. Using combinatorial analysis, they showed that the density of particles was decreasing according to a power law ( $t^{-1/2}$ ) in the case of a symmetric initial velocity distribution. The investigation of this one-dimensional problem was generalized by Droz *et al.* [6] to the three-velocity case, where the initial velocity distribution is given by  $\varphi(v;0) = p_+ \delta(v-c) + p_0 \delta(v) + p_- \delta(v+c)$  with  $p_+ = p_-$  (symmetric case) and  $p_+ + p_0 + p_- = 1$ . It turns out that the decay of the particle density depends on the details of the initial velocity distribution. The following analytical results were obtained. For  $p_0 < 1/4$ , the density  $n(v;t)$  of particles with velocity  $v = \{0, +c, -c\}$ , behaves in the long-time limit as  $n(0;t) \sim t^{-1}$ ,  $n(\pm c;t) \sim t^{-1/2}$ . When  $p_0 = 1/4$ ,  $n(0;t) \sim n(\pm c;t) \sim t^{-2/3}$ . Finally, for  $p_0 > 1/4$ , one finds that  $n(0;t)$  saturates to a nonzero stationary value, while  $n(\pm c;t)$  decays faster than a power law. Moreover, it was shown that in one dimension, annihilation dynamics creates strong correlations between the velocities of colliding particles, which excludes a Boltzmann-like approximation. Pairs of nearest neighbor particles have the tendency to align their velocities and propagate in the same direction [6].

An analytical investigation of the one-dimensional case with a continuous velocity distribution is much more difficult. A dynamical scaling theory, whose validity was supported by extensive numerical simulations for several velocity distributions, led Rey *et al.* [7] to the conjecture that all

the continuous velocity distributions  $\varphi(v)$  that are symmetric, regular and, such that  $\varphi(0) \neq 0$  are attracted in the long-time regime towards the same Gaussian-like distribution, and thus belong to the same universality class.

For higher dimensions, most of the studies are based on an uncontrolled Boltzmann-like description [2,3,11] or numerical simulations [12]. However, based on phenomenological mean-field-like arguments, Krapivsky *et al.* have studied the annihilation kinematics of a bimodal velocity modulus distribution in  $d > 2$  dimensions [4]. In the case of a mixture of moving and motionless particles they showed that the stationary particles always persist, while the density of moving particles decays exponentially. This approach contains unknown phenomenological parameters, and thus a complete comparison with the results obtained by numerical simulation is not possible.

In a recent paper, Piasecki *et al.* [14] gave an analytical derivation of the hierarchy equations obeyed by the reduced distributions for the annihilation dynamics. In dimension  $d > 1$  for a spatially homogeneous system, and in the limit (the so-called Grad limit) for which the particle diameter  $\sigma \rightarrow 0$  and the particle density  $n(t) \rightarrow \infty$ , such that  $n(t)\sigma^{d-1} = \lambda^{-1}$ , where  $\lambda$  is the mean free path, the hierarchy reduces to the Boltzmann-like hierarchy. This hierarchy propagates the factorization of the reduced  $k$ -particle distribution in terms of one-particle distribution functions. Thus, if the initial state is factorized, the whole hierarchy reduces to one nonlinear equation for the one-particle Boltzmann distribution. For annihilation kinetics, the ratio of particle diameter to mean-free path vanishes in the long-time limit, and the situation becomes similar to the Grad limit discussed above for  $\lambda \rightarrow \infty$ . Thus the long-time limit of the annihilation dynamics (for  $d > 1$ ) is likely to be adequately described by the nonlinear Boltzmann equation.

A scaling analysis of the nonlinear Boltzmann equation led to analytical expressions for the exponents describing the decay of the particle density and of the root-mean-square velocity in the case of continuous velocity distributions [14].

In view of the different behaviors observed in one dimension for discrete or continuous velocity distributions, it is

relevant to study the case of distributions with discrete modulus spectrum in dimensions higher than 1. The goal of this paper is to investigate simple examples of this kind in three dimensions for which the nonlinear Boltzmann equation derived in Ref. [14] can be exactly solved. The generalization of this approach to an arbitrary dimension is straightforward, and for the sake of comparison with numerical simulations, we shall also consider the two-dimensional situation in some detail.

The validity of the Boltzmann description in the long-time limit will be confirmed by comparing our analytical predictions with the results obtained by a molecular dynamics simulation.

The paper is organized as follows. In Sec. II we define the model. In Sec. III the three-dimensional Boltzmann equation is solved analytically for a two-velocity modulus ( $c_1$  and  $c_2$ ) isotropic distribution. For simplicity we first consider the one velocity model  $c_1 = c_2 > 0$  that allows to draw interesting comparisons with the same model in one dimension. Then the implicit solution for the particle densities in the general case  $c_1 > c_2 > 0$  is established. It is shown analytically that in the long-time limit the particle densities decay according to power laws, with exponents depending continuously on the value of the velocity modulus ratio. We also find upper and lower bounds to the particle densities that are compared with the numerical solution of the dynamical equation. The particular case of a mixture of moving ( $c_2 > 0$ ) and motionless ( $c_1 = 0$ ) particles is also investigated. It turns out that the particle densities decay exponentially to zero for the moving particles, and to a nonzero value for the motionless ones. This phenomenology is independent of space dimension, and in Sec. IV, it will be shown explicitly to hold in two dimensions by implementing molecular dynamics simulations. This numerical method has the advantage of being free of the approximations underlying Boltzmann's dynamics and, therefore, provides an interesting test for the analytical predictions. Section V contains our interpretations and conclusions.

## II. THE MODEL

We consider a system made of spheres of diameter  $\sigma$  moving ballistically in three-dimensional space. If two particles touch each other, they annihilate and thus disappear from the system. We consider only two-body collisions. The initial spatial distribution of particles is supposed to be uniform, therefore it remains uniform during the evolution. Indeed, if the state is initially translationally invariant, then the free evolution preserves this symmetry. Annihilation dynamics adds the effect of binary collisions that depends only on the distance between particles, thus preserving the translational invariance. Finally, existing numerical simulations seem to be compatible with this assumption of homogeneity [14]. We are interested in the time evolution of the number density of particles with a given velocity modulus.

Let  $f_1(\mathbf{v}; t)$  be the distribution function of the density of particles in  $\mathbb{R}^3$  with velocity  $\mathbf{v} \in \mathbb{R}^3$  at time  $t$ . For spatially homogeneous states, the distribution function has the form

$$f_1(\mathbf{v}; t) = n(t) \varphi(\mathbf{v}; t), \quad (1)$$

where  $\varphi(\mathbf{v}; t)$  is the velocity probability density. In the long-time limit, Piasecki *et al.* [14] have shown that the hierarchy satisfied by the reduced distributions approached the Boltzmann hierarchy. If the initial state is factorized, the nonlinear Boltzmann equation provides then the complete description of annihilation dynamics,

$$\begin{aligned} \frac{\partial}{\partial t} f_1(\mathbf{v}_1; t) &= \sigma^2 \int d\hat{\boldsymbol{\sigma}} \theta(-\hat{\boldsymbol{\sigma}} \cdot \hat{\mathbf{v}}_{12}) (\hat{\boldsymbol{\sigma}} \cdot \hat{\mathbf{v}}_{12}) \\ &\times \int_{\mathbb{R}^3} d\mathbf{v}_2 |\mathbf{v}_{12}| f_1(\mathbf{v}_1; t) f_1(\mathbf{v}_2; t). \end{aligned} \quad (2)$$

Here  $\theta$  is the Heaviside function,  $\mathbf{v}_{12} = \mathbf{v}_1 - \mathbf{v}_2$  the relative velocity of two particles,  $\hat{\mathbf{v}}_{12} = \mathbf{v}_{12}/v_{12}$  a unit vector,  $v_{12} = |\mathbf{v}_{12}|$ , and the integration with respect to  $d\hat{\boldsymbol{\sigma}}$  is the angular integration over the solid angle.

We consider spherically symmetric initial conditions  $f_1(v; 0)$ ,  $v = |\mathbf{v}|$ . This symmetry property is propagated by the dynamics. The Boltzmann equation (2) then takes the form

$$\begin{aligned} \frac{\partial}{\partial t} f_1(v; t) &= -\frac{2}{3} (\pi\sigma)^2 f_1(v; t) \int_0^\infty du u^2 f_1(u; t) \\ &\times \left[ \frac{(u+v)^3 - |u-v|^3}{uv} \right]. \end{aligned} \quad (3)$$

Equation (3) is a nonlinear homogeneous integral equation for the distribution function  $f_1(v; t)$ . A simplification arises if the initial velocity distribution has a discrete modulus spectrum. This spectrum is preserved by the annihilation dynamics as no new velocities are created. A simple case is provided by the bimodal distribution

$$\varphi(v, 0) = \frac{A}{4\pi c_1^2} \delta(v - c_1) + \frac{1-A}{4\pi c_2^2} \delta(v - c_2), \quad (4)$$

where  $c_2 > c_1 \geq 0$  and  $A$  denotes the fraction of particles with velocity modulus  $c_1$ .

## III. EXACT RESULTS

Before addressing the general case, we first consider the single-species problem where  $c_2 = c_1 > 0$ .

### A. Single-velocity modulus distribution

Setting  $c_2 = c_1 = c > 0$  in Eq. (4), one obtains from Eq. (1)

$$f_1(v; t) = n(t) \frac{1}{4\pi c^2} \delta(v - c). \quad (5)$$

From the kinetic equation (3), we find

$$\frac{d}{dt} n(t) = -\frac{4}{3} \pi \sigma^2 c n(t)^2, \quad (6)$$

whose solution is

$$n(t) = \frac{n_0}{1 + \frac{4}{3} \pi \sigma^2 n_0 c t}, \quad (7)$$

where  $n(0) = n_0$ . A striking observation is that, in the limit  $t \rightarrow \infty$ , the density (7) becomes independent of its initial value  $n_0$ . Note that the same phenomenon is also present for simple diffusion limited annihilation such as  $A + A \rightarrow 0$ , when the dimension of the system is larger than 2 [16].

Contrary to the one-dimensional case for which it has been rigorously shown that the density decays proportionally to  $t^{-1/2}$  [1], one sees from Eq. (7) that in three dimensions, Boltzmann's dynamics is faster as the density decays according to  $t^{-1}$ , which is the mean-field value [4]. We note, however, that the same behavior  $n(t) \propto 1/t$  holds in all dimensions within Boltzmann's kinetic theory (and in fact, more generally within the framework of a scaling analysis of the hierarchy governing the dynamics of ballistic annihilation [14]). This discrepancy between Boltzmann's prediction and the exact result in one dimension illustrates the crucial importance of dynamical correlations when  $d = 1$ . On the other hand, as suggested in Ref. [14] and explicitly shown below by molecular dynamics simulations, the nonlinear Boltzmann equation is relevant for describing the long-time dynamics of ballistic annihilation when  $d \geq 2$ . In this case the particles are very diluted and no dynamical correlations can develop during the time evolution, which would violate the molecular chaos hypothesis.

### B. Mixture of particles with two nonzero velocity moduli

Consider the case where particles with velocities  $c_1 > 0$  and  $c_2 > c_1$  are initially present. Thus  $f_1(v; t)$  is of the form

$$f_1(v; t) = X(t) \frac{1}{4\pi c_1^2} \delta(v - c_1) + Y(t) \frac{1}{4\pi c_2^2} \delta(v - c_2), \quad (8)$$

where  $X(t)$  and  $Y(t)$  are, respectively, the densities of particles with velocities  $c_1$  and  $c_2$ . They add up to the total density  $X(t) + Y(t) = n(t)$ . Upon rescaling the time according to  $\tau = t c_2 \pi \sigma^2 / 3$ , it follows from Eq. (3) that

$$\dot{X}(\tau) = -4\gamma X(\tau)^2 - (3 + \gamma^2) X(\tau) Y(\tau), \quad (9a)$$

$$\dot{Y}(\tau) = -4Y(\tau)^2 - (3 + \gamma^2) X(\tau) Y(\tau), \quad (9b)$$

where  $0 \leq \gamma = c_1/c_2 < 1$ , and the overdot denotes time derivative with respect to  $\tau$ .

The set of equations (9) is a nonlinear homogeneous system of coupled differential equations with constant coefficients. An implicit solution can be obtained by introducing the function  $V(\tau)$  defined as  $V(\tau) = Y(\tau)/X(\tau)$ . From Eq. (9) we get

$$\frac{dY}{dX} = \frac{4V^2 + (3 + \gamma^2)V}{4\gamma + (3 + \gamma^2)V}, \quad (10)$$

so that

$$\frac{dX}{X} = \frac{4\gamma + (3 + \gamma^2)V}{(1 - \gamma^2)V^2 + (1 - \gamma)(3 - \gamma)V} dV. \quad (11)$$

Integrating Eq. (11) yields

$$\frac{X_0}{X} = \left( \frac{V_0}{V} \right)^\alpha \left( \frac{V_0 + \frac{3 - \gamma}{1 + \gamma}}{V + \frac{3 - \gamma}{1 + \gamma}} \right)^\beta, \quad (12)$$

with  $\alpha = 4\gamma / [(1 - \gamma)(3 - \gamma)] \geq 0$ ,  $\beta = (3 + \gamma^2) / (1 - \gamma^2) - \alpha > 0$ ,  $V(0) = V_0 = Y_0/X_0$ ,  $X_0 = X(0)$ ,  $Y_0 = Y(0)$ . The special case of  $\gamma = 0$  will be discussed in Sec. III C, hence from now on we assume that  $\gamma > 0$ , so that  $\alpha > 0$ . Equations (9) can also be written as

$$\frac{d}{d\tau} \left( \frac{1}{X} \right) = 4\gamma + (3 + \gamma^2) \frac{Y(\tau)}{X(\tau)}, \quad (13a)$$

$$\frac{d}{d\tau} \left( \frac{1}{Y} \right) = 4 + (3 + \gamma^2) \frac{X(\tau)}{Y(\tau)}. \quad (13b)$$

Multiplying the right-hand side (RHS) of Eq. (13a) by  $X_0$  and equating it with the derivative of the RHS of Eq. (12), one obtains upon integration from 0 to  $\tau$  the relation

$$X_0 \tau = \int_V^{V_0} du \frac{1}{4\gamma + (3 + \gamma^2)u} \times \left\{ -\frac{d}{du} \left[ \left( \frac{V_0}{u} \right)^\alpha \left( \frac{V_0 + \frac{3 - \gamma}{1 + \gamma}}{u + \frac{3 - \gamma}{1 + \gamma}} \right)^\beta \right] \right\}. \quad (14)$$

Equation (14) implicitly defines the time dependence of the function  $V(\tau)$ . The procedure to obtain the densities  $X(\tau)$  and  $Y(\tau)$  from Eq. (14) is as follows. The integration in Eq. (14) leads to Appel functions, which may be inverted (at least numerically) in order to give  $V(\tau)$ . The insertion of  $V(\tau)$  in Eq. (12) then gives  $X(\tau)$ . It is then straightforward to obtain  $Y(\tau)$ , having determined  $V(\tau)$  and  $X(\tau)$ . The structure of the implicit relation (14) permits us to establish interesting analytical results.

First, let us investigate the long-time behavior of the particle densities  $X(\tau)$  and  $Y(\tau)$ . When  $\tau \rightarrow \infty$ , the LHS of Eq. (14) diverges linearly, which implies that  $\lim_{\tau \rightarrow \infty} V(\tau) = 0$ . So, in the long-time limit, the implicit relation (14) leads to the asymptotic formula

$$X_0 \tau \simeq \frac{1}{4\gamma} \left( \frac{V_0}{V} \right)^\alpha \left( \frac{1 + \gamma}{3 - \gamma} V_0 + 1 \right)^\beta, \quad (15)$$

so that

$$V(\tau) \approx V_0 \left( \frac{1+\gamma}{3-\gamma} V_0 + 1 \right)^{\beta/\alpha} (4\gamma X_0 \tau)^{-1/\alpha}. \quad (16)$$

As  $\lim_{\tau \rightarrow 0} V(\tau) = 0$ , Eq. (13a) takes the asymptotic form  $d/d\tau(1/X) = 4\gamma$ . Hence we conclude that

$$X(\tau) \approx \frac{1}{4\gamma} \tau^{-1}. \quad (17)$$

On the other hand, from Eqs. (13b) and (16) we find the long-time relation

$$\frac{d}{d\tau} \left( \frac{1}{Y} \right)^{\tau \rightarrow \infty} \approx (3+\gamma^2) \frac{1}{V_0} \left( \frac{1+\gamma}{3-\gamma} V_0 + 1 \right)^{-\beta/\alpha} (4\gamma X_0 \tau)^{1/\alpha}, \quad (18)$$

which upon integration yields

$$Y(\tau) \approx \frac{\tau \rightarrow \infty V_0}{4\gamma} (4\gamma X_0)^{-1/\alpha} \left( \frac{1+\gamma}{3-\gamma} V_0 + 1 \right)^{\beta/\alpha} \tau^{-(3+\gamma^2)/4\gamma}. \quad (19)$$

Note that the exponent for the density  $Y(\tau)$  is a function of the ratio  $\gamma = c_1/c_2$  and thus is nonuniversal. In the limit  $\gamma \rightarrow 1$  one recovers the asymptotic behavior of the single-velocity modulus distribution (see Sec. III A).

Second, we may find analytical upper and lower bounds for  $X(\tau)$  and  $Y(\tau)$ . Granted that  $\alpha > 0$  and  $\beta > 0$ , the integrand of Eq. (14) is a strictly monotonic decreasing positive function of  $u$ , therefore  $V(\tau) < V_0$  for all  $\tau > 0$ . Considering that  $(4\gamma)^{-1} \geq [4\gamma + (3+\gamma^2)u]^{-1}$  for  $u \geq 0$ , the insertion of Eq. (12) in Eq. (14) provides the inequality  $X_0 \tau \leq (X_0/X - 1)/4\gamma$  which leads to an upper bound for  $X(\tau)$ . On the other hand, the inequality  $[4\gamma + (3+\gamma^2)u]^{-1} \leq [4\gamma + (3+\gamma^2)V_0]^{-1}$  yields a lower bound, so that we finally get

$$\frac{X_0}{1 + [4\gamma X_0 + (3+\gamma^2)Y_0]\tau} \leq X(\tau) \leq \frac{X_0}{1 + 4\gamma X_0 \tau}. \quad (20)$$

Note that for times such that

$$4\gamma X_0 \tau \gg 1, \quad (21)$$

the upper bound (20) coincides with the exact asymptotic relation (17). The same kind of analysis as that leading to Eq. (20) yields the upper bound,

$$0 \leq Y(\tau) \leq \frac{Y_0}{1 + (3+\gamma^2)X_0 \tau}. \quad (22)$$

The width defined by the difference of the bounds in both cases (20) and (22) is  $\mathcal{O}(\tau^{-1})$ . Figures 1 and 2 show the numerical solution for  $X(\tau)$ ,  $Y(\tau)$ , the bounds (20) and (22), as well as their asymptotic behaviors (17) and (19) on a logarithmic scale.

The knowledge of the numerical solution (see Figs. 1 and 2) allows to determine the crossover time, separating the early and long-time (power law) regimes.

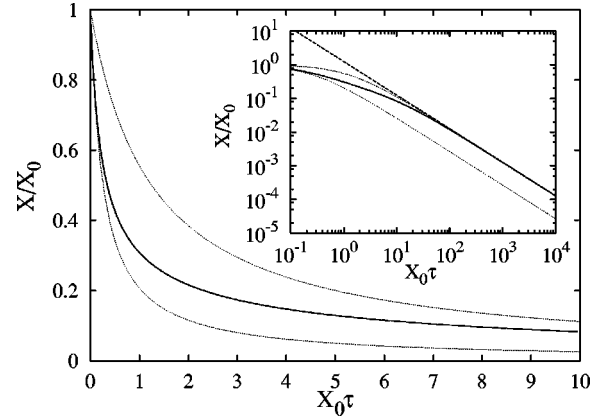


FIG. 1. Upper and lower bounds (20) (dotted lines) as well as the numerical solution of the set of equations (9) for  $X(\tau)$  with  $X_0 = Y_0$ ,  $\gamma = 0.2$  (continuous line). The inner logarithmic plot shows indeed the power law behavior  $X(\tau) \sim \tau^{-1}$  for  $\tau \rightarrow \infty$ , where the asymptotic solution (17) is represented by the dashed straight line. Moreover, in this regime the solution converges to the upper bound (20).

### C. Mixture of moving and motionless particles

We now consider a particular case of Sec. III B that we solve exactly in the asymptotic limit  $\tau \rightarrow \infty$ . The system is now characterized by a certain number of motionless particles (zero velocity,  $c_1 = 0$ ), whereas the rest of the particles have a given nonzero velocity modulus. Thus, setting  $\gamma = 0$  in Eq. (12), inverting the relation in order to find  $V = V(X)$ , then making use of Eq. (13a) with  $\gamma = 0$  leads to

$$\frac{d}{d\tau} \left( \frac{1}{X} \right) = 3 \left( 3 + \frac{Y_0}{X_0} \right) \left( \frac{X}{X_0} \right)^{1/3} - 9. \quad (23)$$

The integration of Eq. (23) yields

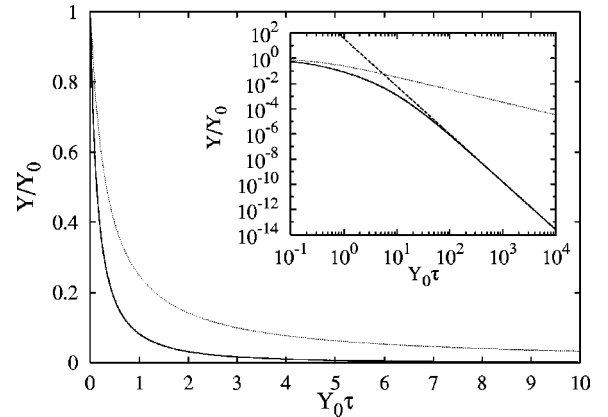


FIG. 2. Upper bound (22) (dashed lines) as well as the numerical solution of the set of equations (9) for  $Y(\tau)$  with  $X_0 = Y_0$ ,  $\gamma = 0.2$  (continuous line). The inner logarithmic plot of the numerical solution shows indeed the power law behavior  $Y(\tau) \sim \tau^{-(3+\gamma^2)/4\gamma}$  for  $\tau \rightarrow \infty$ , where the asymptotic solution (19) is represented by the dashed straight. Furthermore, the use of both the upper bound (17) and the asymptotic form (19) allows one to find an analytical approximation for  $Y(\tau)$ , which turns out to be exact in both limits  $\tau \rightarrow 0$  and  $\tau \rightarrow \infty$ .

$$3X_0\tau = \frac{1}{3}\left[1 - \frac{X_0}{X}\right] + \frac{a}{2}\left[1 - \left(\frac{X_0}{X}\right)^{2/3}\right] + a^2\left[1 - \left(\frac{X_0}{X}\right)^{1/3}\right] + a^3 \ln\left[\frac{a-1}{a - (X_0/X)^{1/3}}\right], \quad (24)$$

with  $a = 1 + Y_0/3X_0$ . In the asymptotic limit  $\tau \rightarrow \infty$ , the LHS of Eq. (24) tends to  $+\infty$ . The density  $X(\tau)$  cannot thus tend to zero, and must approach a strictly positive value  $X(\infty) = X_\infty > 0$ . For  $\tau \rightarrow \infty$ , all terms on the RHS of Eq. (24) but the logarithmic one approach a finite limit. This implies the asymptotic behavior

$$X_\infty = \lim_{\tau \rightarrow \infty} X(\tau) = \frac{X_0}{a^3} = X_0 \left(\frac{3X_0}{3X_0 + Y_0}\right)^3 > 0. \quad (25)$$

Replacing  $X$  by  $X_\infty$  in all terms of Eq. (24) except the logarithmic one and then inverting the relation  $\tau(X)$ , we find

$$X(\tau) \approx X_\infty [1 - \varepsilon(X_0, Y_0; \tau)]^{-3} \approx X_\infty [1 + 3\varepsilon(X_0, Y_0; \tau)], \quad (26)$$

where

$$\varepsilon(X_0, Y_0; \tau) = \frac{Y_0 \exp(\mu/a^3)}{3X_0 + Y_0} \exp(-3X_\infty\tau) \quad (27)$$

and  $\mu = 1/3 + a/2 + a^2 - 11a^3/16 < 0$ . Making use of Eq. (9a) with  $\gamma = 0$ , we find

$$Y(\tau) \approx 3X_\infty \varepsilon(X_0, Y_0; \tau). \quad (28)$$

Hence we have

$$X(\tau) \approx X_\infty + Y(\tau). \quad (29)$$

There is a qualitative difference from the case  $c_1 > 0$ . As shown in Fig. 3, the density of particles at rest approaches the asymptotic value  $X_\infty > 0$  exponentially fast, while the density of moving particles goes to zero exponentially. Table I summarizes the long-time behavior for the different cases.

Note that generalizing our results to any dimension  $d \geq 2$  is straightforward (see below for the case  $d = 2$ ). The algebraic or exponential decay of the particle densities hold irrespective of  $d$ . In particular, for the general case  $c_1 > 0$  the exponent of the density of ‘‘slow’’ particles is independent of  $d$  so that asymptotically  $X(\tau) \sim \tau^{-1}$ . Finally the relation (29) still holds.

#### IV. COMPARISON WITH NUMERICAL SIMULATIONS

The analytical predictions obtained in the preceding section rely on the validity of the molecular chaos assumption, leading to the Boltzmann equation. It is therefore instructive to compare these predictions to the results of molecular dynamics (MD) simulations, where the exact equations of mo-

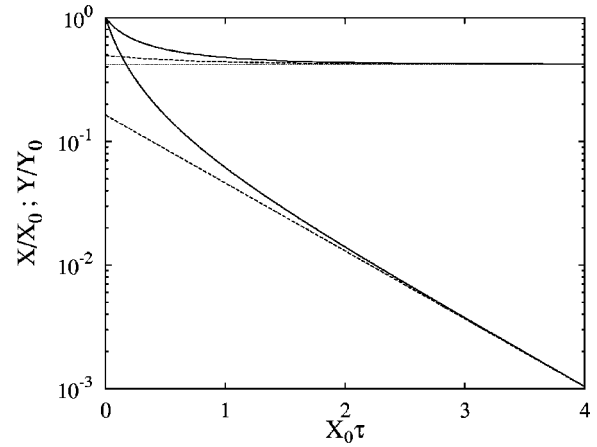


FIG. 3. Linear-logarithmic plot of the numerical solution of the set of equations (9) for  $X_0 = Y_0$ ,  $\gamma = 0$  (continuous lines). The asymptotic relations (26) and (28) are shown by the dashed lines, and the asymptotic limit (25) by the dotted line.

tion of the particles are integrated (see Ref. [14] for more details concerning the method).

#### A. Analytical results in two dimensions

MD simulations are most efficiently performed in two dimensions, where the best statistical accuracy can be achieved. We consequently repeat the analysis of Secs. II and III for a two-dimensional system. Introducing the rescaled time  $\tau = 2\pi\sigma c_2 t$ , one obtains the counterpart of Eqs. (9) in the form

$$\dot{X}(\tau) = -4\gamma X(\tau)^2 - \kappa(\gamma)X(\tau)Y(\tau), \quad (30a)$$

$$\dot{Y}(\tau) = -4Y(\tau)^2 - \kappa(\gamma)X(\tau)Y(\tau), \quad (30b)$$

where  $\kappa(\gamma) = \int_0^\pi d\varphi \sqrt{1 + \gamma^2 - 2\gamma \cos \varphi}$ . In the limit  $\tau \rightarrow \infty$ , the solution of the system (30) reads

$$X(\tau) \approx \frac{1}{4\gamma} \tau^{-1}, \quad (31a)$$

$$Y(\tau) \approx \frac{V_0}{4\gamma} (4\gamma X_0)^{-1/\mu} \left(\frac{4 - \kappa}{\kappa - 4\gamma} V_0 + 1\right)^{\nu/\mu} \tau^{-\kappa/4\gamma}, \quad (31b)$$

where  $\mu = 4\gamma/(\kappa - 4\gamma)$  and  $\nu = \kappa/(4 - \kappa) - \mu$ . On the other hand, taking the limit  $\gamma \rightarrow 0$  in Eqs. (30) and solving the corresponding system leads to the long-time behavior

TABLE I. Summary of the long-time density behavior in three dimensions.

	$c_2 = c_1 > 0$	$c_2 > c_1 \neq 0$	$c_2 > c_1 = 0$
$X(\tau)$	$\tau^{-1}$	$\tau^{-1}$	$X_\infty [1 + 3 \exp(-3X_\infty\tau)]$
$Y(\tau)$	$\tau^{-1}$	$\tau^{-(3+\gamma^2)/4\gamma}$	$X_\infty 3 \exp(-3X_\infty\tau)$

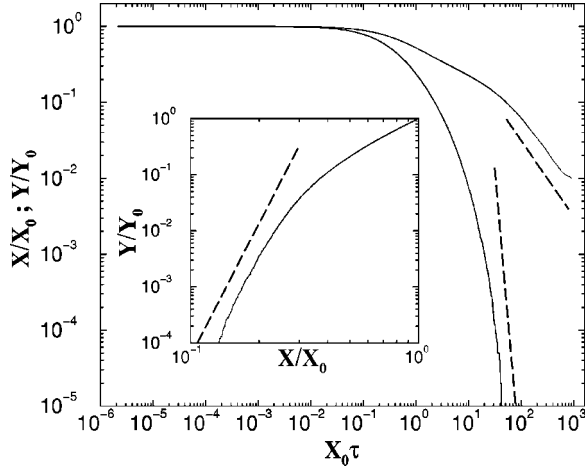


FIG. 4. Log-log plot of the densities  $X$  (upper curve) and  $Y$  (lower curve) as a function of rescaled time, as obtained in the MD simulations of a two-dimensional system with  $\gamma=0.1$ . The initial condition corresponds to an equimolar mixture ( $X_0=Y_0$ ) of  $N=2 \times 10^5$  particles, with reduced density  $(X_0+Y_0)\sigma^2=0.1$  at  $\tau=0$  (both species have the same diameter). The dashed lines have slopes  $-1$  and  $-7.9$  [as predicted by Eqs. (31)]. Inset: log-log plot of  $Y$  as a function of  $X$ , where the broken line has slope  $-7.9$ .

$$X(\tau) \approx X_\infty [1 + \varepsilon_2(X_0, Y_0; \tau)], \quad (32a)$$

$$Y(\tau) \approx X_\infty \varepsilon_2(X_0, Y_0; \tau), \quad (32b)$$

where

$$\frac{X_\infty}{X_0} = \frac{1}{(1 + V_0\chi)^{1/\chi}} \quad (33)$$

and  $\chi=4/\pi-1$ . In Eqs. (32), we have

$$\begin{aligned} \varepsilon_2(X_0, Y_0; \tau) &= \pi V_0^{(1+V_0\chi)^{-1/\chi-1}} \exp(-JX_\infty/X_0) \\ &\quad \times \exp(-\pi X_\infty \tau), \end{aligned} \quad (34)$$

and

$$J = \int_0^{V_0} du \ln(u) \left[ -\frac{d^2}{du^2} \left( \frac{1/\chi + V_0}{1/\chi + u} \right)^{1/\chi} \right]. \quad (35)$$

### B. Molecular dynamics simulations

MD simulations have been implemented with systems of typically  $N=10^5$  to  $4 \times 10^5$  spheres in two dimensions (discs). Periodic boundary conditions were enforced, and low densities considered, in order to minimize the excluded volume effects discarded at the Boltzmann level (note that these effects are necessarily transient since the density decreases with time).

Figure 4 compares the MD results obtained with  $\gamma=1/10$  to the predictions of Eqs. (31) (for  $\gamma=1/10$ , the time

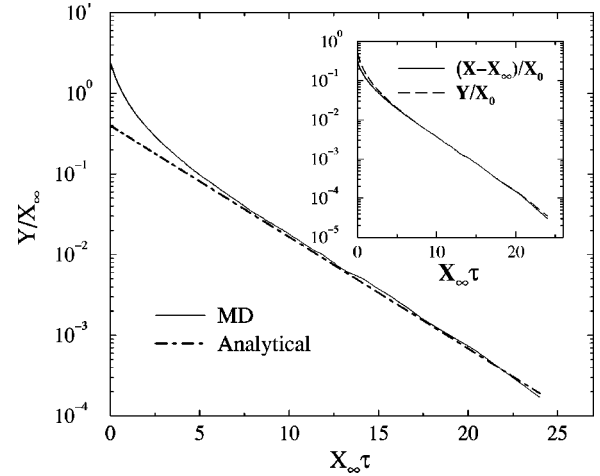


FIG. 5. Linear-logarithmic plot of the density of moving particles. Here,  $\gamma=0$ ,  $X_0=Y_0=5 \times 10^{-3}/\sigma^2$  [corresponding to a very low total initial packing fraction  $\eta_0 \equiv \pi(X_0+Y_0)\sigma^2/4=0.0078$ ]. The initial number of particles is  $N=4 \times 10^5$ . The results of MD simulations (continuous curve) are compared to the predictions of Eqs. (32), shown by the broken line. The inset shows that  $X-X_\infty$  and  $Y$  (obtained in MD) have asymptotically the same time decay [see Eqs. (32)].

decay of the “fast” particles is governed by the exponent  $\kappa/4\gamma \approx 7.9$ ). Although the large-time behaviors for  $X$  and  $Y$  are compatible with those given by Eqs. (31), it may be observed that the corresponding asymptotic regime is difficult to probe, even for large systems. The parametric plot [or “trajectory”  $Y(X)$ ] shown in the inset is however in agreement with the relation  $Y \propto X^{\kappa/4\gamma}$  deduced from Eq. (31).

We have also performed MD simulations for a mixture of moving and motionless particles ( $\gamma=0$ ), where it is expected that the density  $X$  of particles at rest decreases down to a nonvanishing value  $X_\infty$ . In the situation of an equimolar mixture ( $X_0=Y_0$ ), we have  $V_0=1$ , so that according to Eq. (33),  $X_\infty/X_0 \approx 0.414$ . The MD simulations are in agreement with this scenario, and we find  $X_\infty/X_0 \approx 0.408$  irrespective of the initial conditions for a system with initially  $N=2 \times 10^5$  particles. The results for the time dependence of  $X$  and  $Y$  are displayed in Fig. 5. We conclude that the numerical simulations are again in agreement with the prediction of Boltzmann’s kinetic theory.

### V. CONCLUSIONS

We have shown that for some simple spatially homogeneous systems, characterized by a velocity distribution with a discrete velocity modulus spectrum, it is possible to find the exact solution for the nonlinear integral equation describing the dynamics of ballistic annihilation. These results, obtained at the level of a Boltzmann equation, have been validated by explicit comparison with molecular dynamics simulations in two dimensions.

For a single-velocity modulus distribution, the particle density of the model decays asymptotically as  $n(t) \sim t^{-1}$ , irrespective of space dimension. It was however rigorously

shown that in one dimension, the decay is slower,  $n(t) \sim t^{-1/2}$ . This difference is a consequence of the fact that in one dimension strong dynamical correlations are created [6], which invalidate the approximation underlying Boltzmann's dynamics. In higher dimensions, the Boltzmann equation becomes exact in the long-time limit.

In the case of a distribution with two different finite non-zero velocity moduli, we found that both particle densities decay for a large time according to a power law. The interesting feature is that the density of the slow particles decays as  $t^{-1}$ , while the density of the fast particles decays more rapidly (e.g., as  $t^{-(3+\gamma^2)/4\gamma}$  in three dimensions), with a non-universal exponent depending continuously on the velocity modulus ratio  $\gamma=c_1/c_2$ . A rough criterion for the crossover time separating the short- and long-time regimes has been given in Eq. (21).

Finally, the case  $c_1=0$  leads to a particularly interesting behavior. Independently of the initial conditions, the densities of the moving and the motionless particles both decrease exponentially fast, however down to a nonzero value for particles at rest. This behavior is quite different from that observed in the one-dimensional case where the initial value of the density of motionless particles plays an important role in the long-time regime. This difference between one dimension and higher dimensions reflects once again the important role played by the dynamically created correlations for  $d=1$ .

The case with motionless particles can be viewed as a

problem of ballistic annihilation of particles with one-velocity moduli moving in a random medium containing immobile traps (the motionless particles) that can capture a moving particle and then disappear. Here again, the situation can be compared to similar problems in diffusion limited annihilation, where the presence of traps can modify the long-time dynamics from a power law to an exponential decay [17].

It would be interesting to compare the above theoretical predictions with some experimental data. Besides growth and coarsening problems, ballistic annihilation could model other physical systems such as, for example, the fluorescence of laser excited gas atoms with quenching on contact [18]. However, the correspondence between such experimental situations and our model is not yet close enough to allow comparison. We would be highly interested in the knowledge of other physical systems that could be described by the models studied here.

#### ACKNOWLEDGMENTS

This work was partially supported by the Swiss National Science Foundation. M.D. acknowledges the support of the Swiss National Science Foundation and of the CNRS. J.P. acknowledges the hospitality at the Department of Physics of the University of Geneva. We thank P. L. Krapivsky for bringing our attention to Ref. [4].

- 
- [1] Y. Elskens and H.L. Frisch, *Phys. Rev. A* **31**, 3812 (1985).
  - [2] E. Ben-Naim, S. Redner, and F. Leyvraz, *Phys. Rev. Lett.* **70**, 1890 (1993).
  - [3] E. Ben-Naim, P.L. Krapivsky, F. Leyvraz, and S. Redner, *J. Phys. Chem.* **98**, 7284 (1994).
  - [4] P.L. Krapivsky, S. Redner, and F. Leyvraz, *Phys. Rev. E* **51**, 3977 (1995).
  - [5] J. Piasecki, *Phys. Rev. E* **51**, 5535 (1995).
  - [6] M. Droz, P.A. Rey, L. Frachebourg, and J. Piasecki, *Phys. Rev. Lett.* **75**, 160 (1995); *Phys. Rev. E* **51**, 5541 (1995).
  - [7] P.A. Rey, M. Droz, and J. Piasecki, *Phys. Rev. E* **57**, 138 (1997).
  - [8] P.A. Rey, M. Droz, and J. Piasecki, *Phys. Rev. E* **59**, 126 (1998).
  - [9] Y. Kafri, *J. Phys. A* **33**, 2365 (1999).
  - [10] R.A. Blythe, M.R. Evans, and Y. Kafri, *Phys. Rev. Lett.* **85**, 3750 (2000).
  - [11] P.L. Krapivsky and C. Sire, *Phys. Rev. Lett.* **86**, 2494 (2001).
  - [12] B. Chopard, A. Masselot, and M. Droz, *Phys. Rev. Lett.* **81**, 1845 (1998).
  - [13] E. Trizac, *Phys. Rev. Lett.* **88**, 160601 (2002).
  - [14] J. Piasecki, E. Trizac, and M. Droz, *Phys. Rev. E* **66**, 066111 (2002).
  - [15] J. Krug and H. Spohn, *Phys. Rev. A* **38**, 4271 (1988).
  - [16] D. Toussain and F. Wilczek, *J. Chem. Phys.* **78**, 2642 (1983).
  - [17] M.D. Donsker and S.R.S. Varadhan, *Commun. Pure Appl. Math.* **28**, 525 (1975).
  - [18] J. Piasecki, P.-A. Rey, and M. Droz, *Physica A* **229**, 515 (1996).